DALTON PERSPECTIVE

Spin state tuning of non-heme iron-catalyzed hydrocarbon oxidations: participation of Fe^{III}–OOH and Fe^{V}=O intermediates †

Kui Chen, Miquel Costas and Lawrence Que, Jr.

Department of Chemistry and Center for Metals in Biocatalysis University of Minnesota, 207 Pleasant St. SE, Minneapolis, MN, USA. E-mail: que@chem.umn.edu

Received 24th September 2001, Accepted 10th October 2001
First published as an Advance Article on the web 24th January 2002

We have found a family of non-heme iron complexes $[Fe^{II}(L)(CH_3CN)_2]$ (L = tetradentate pyridine containing ligand) with *cis* labile sites that catalyze highly stereoselective hydrocarbon oxidations using H_2O_2 as oxidant. The hydrocarbon oxidation reactivity patterns of this family of catalysts divide them into two subgroups: Category A catalysts which carry out highly stereoselective alkane hydroxylation, olefin epoxidation, and olefin *cis*-dihydroxylation *via* low-spin Fe^{III}–OOH, Fe^{V}=O intermediates and category B catalysts which form high-spin Fe^{III}–OOH intermediates and strongly favor olefin *cis*-dihydroxylation in which both diol oxygen atoms derive from H_2O_2. 6-Methyl substituents on the ligands play an important role in tuning the spin states of the iron centers to afford a family of non-heme iron complexes that catalyze a remarkable array of hydrocarbon oxidation reactions.

1 Introduction

The oxygen activation mechanisms for hydrocarbon oxidations catalyzed by iron centers in enzymes has been a subject of persistent interest in bioinorganic chemistry.[1–5] There are iron enzymes that carry out alkane hydroxylation, olefin epoxidation and olefin *cis*-dihydroxylation. The first two transformations are catalyzed by both heme (*e.g.* cytochrome P450[4]) and non-heme iron enzymes (*e.g.* methane monooxygenase[2]), while *cis*-dihydroxylation is thus far the exclusive function of the non-heme iron containing Rieske dioxygenases, which attack arene double bonds in the first step of the arene biodegradation pathway in soil.[6]

The large amount of information derived from extensive investigations on cytochrome P450 has made it the paradigm for O_2 activation by iron enzymes (Scheme 1).[4,7] Key intermediates in its mechanism of action are (porphyrin)Fe^{III}–OOH and (porphyrin radical)Fe^{IV}=O species, both of which are implicated in alkane hydroxylation and olefin epoxidation reactions.[8–13] Despite the absence of the porphyrin ligand, the proposed mechanisms for non-heme iron enzymes generally follow the heme paradigm. Iron(III)-peroxo and high-valent iron-oxo intermediates have also been observed for methane monooxygenase (MMO),[14,15] an enzyme with an $Fe_2(His)_2(O_2CR)_4$ active site.[16,17] The analogue for the (porphyrin radical)Fe^{IV}=O oxidant in the MMO cycle is an $Fe^{IV}_2(\mu\text{-}O)_2$ intermediate,[18] with the second Fe^{IV} replacing the oxidized porphyrin ligand in providing the oxidizing power needed to carry out alkane hydroxylation and olefin epoxidation.

Rieske dioxygenases constitute a novel class of enzymes that catalyze the incorporation of the two atoms of O_2 into an arene C–C double bond in a *cis* stereochemistry.[19] These enzymes can also carry out hydroxylation of aliphatic C–H bonds and

† Based on the presentation given at Dalton Discussion No. 4, 10–13th January 2002, Kloster Banz, Germany.

Kui Chen received her Ph.D. from the University of Minnesota in 2000 and is currently a postdoctoral associate in the laboratory of Professor T. V. O'Halloran at Northwestern University.

Miquel Costas received his Ph.D. from the Universitat de Girona (Spain) in 1999 and is currently working as a postdoctoral associate in the laboratory of Professor L. Que.

Lawrence Que, Jr. received his Ph.D. from the University of Minnesota in 1973 and is currently on its staff as 3M/Alumni Distinguished Professor of Chemistry. He employs synthetic and biophysical approaches to uncover the principles by which non-heme iron centers in biology activate dioxygen and catalyze novel organic transformations.

Kui Chen

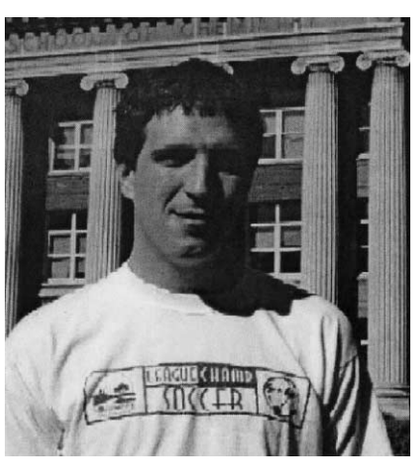

Miquel Costas

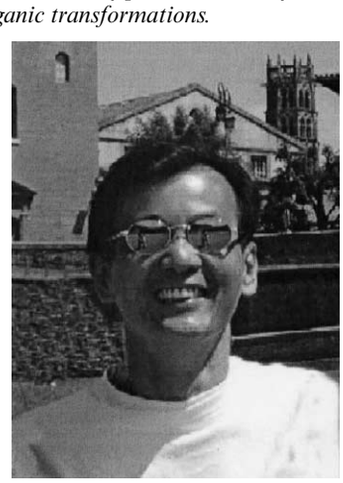

Lawrence Que, Jr.

 DOI: 10.1039/b108629d

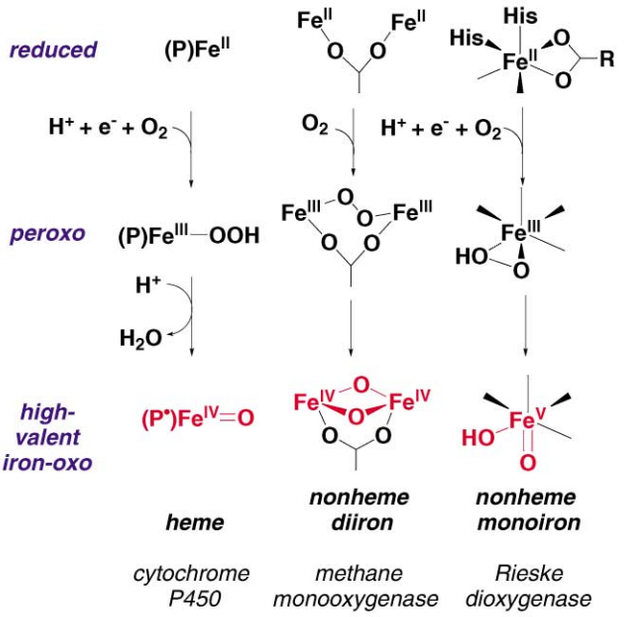

Scheme 1 Unified mechanistic scheme for dioxygen activating iron enzymes.

cis-dihydroxylation of olefinic C–C bonds. The crystal structure of naphthalene 1,2-dioxygenase shows a mononuclear iron center that is coordinated by two histidines and a bidentate carboxylate group, with two adjacent coordination sites available for exogenous ligand binding.[20] To date no intermediates have been detected in the catalytic cycle of these enzymes, but iron(III)-peroxo and iron(V)-oxo species have been proposed as the possible oxidizing species.[3,21]

In the course of developing functional models for non-heme iron oxygenases, we have discovered a family of iron complexes (Scheme 2) that are capable of catalyzing stereospecific hydro-

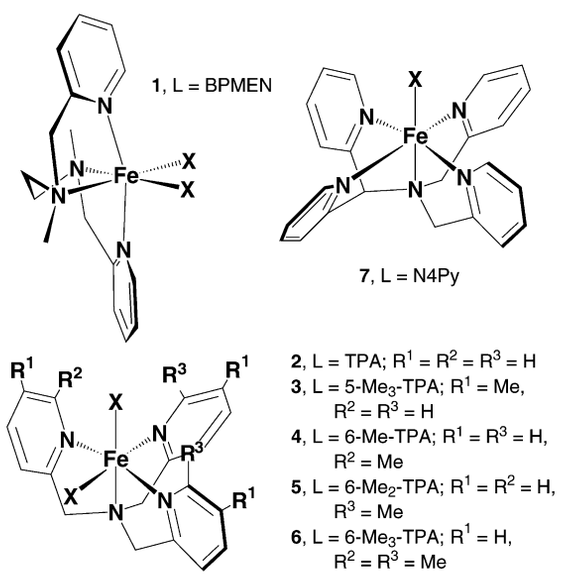

Scheme 2 Structures of iron catalysts discussed in this paper.

carbon oxidations with H_2O_2 as the oxidant, including alkane hydroxylation, olefin epoxidation, and olefin *cis*-dihydroxylation.[22–27] Two key points emerge from the systematic study we have carried out: a) that an iron center with two *cis* labile sites is required to effect this novel chemistry and b) that a formally Fe^{V}=O species can be formed from an Fe^{III}–OOH precursor during the catalytic cycle and is involved in the stereospecific transformations observed.

2 The catalyst family

Our family of catalysts is derived from ligands with the TPA and BPMEN frameworks (Scheme 2). TPA is the tetradentate tripodal tris(2-pyridylmethyl)amine ligand and BPMEN is the linear tetradentate *N*,*N*′-dimethyl-*N*,*N*′-bis(2-pyridylmethyl)-1,2-diaminoethane ligand. The series of iron(II) complexes we have synthesized for this effort, many of which have been crystallographically characterized, can be formulated as $[Fe^{II}(L)(CH_3CN)_2]^{2+}$ complexes, where the tetradentate ligand L occupies four sites of the iron coordination sphere such that the two remaining sites occupied by solvent molecules are oriented *cis* to each other (Scheme 2).[24,26,28] The parent ligands TPA and BPMEN form low-spin iron(II) complexes, as deduced from their crystal structures and NMR spectra; Fe–N bond lengths average 2.0 Å and the NMR features are sharp and span a range of 10 ppm, indicative of a diamagnetic compound. However the introduction of even one 6-methyl group generates sufficient steric hindrance in the vicinity of the iron(II) center to convert it to the high-spin state. Thus crystal structures of 6-methyl substituted complexes have Fe–N bond lengths that average 2.2 Å, and observable NMR features span a range of over 130 ppm. As will be made clear in the discussion below, the spin state of the iron center plays an important role in the reaction mechanism and has a dramatic effect on the course of the catalytic oxidations.

3 Alkane hydroxylation

A typical reaction consists of introducing 10 equivalents of H_2O_2 to an acetonitrile solution of catalyst with a 1000-fold excess of substrate at room temperature in air.[22,24,26] The oxidant is delivered by syringe pump over a 30 minute period to suppress H_2O_2 disproportionation and enhance its conversion to organic products, and iodometry shows that all of the oxidant is consumed at the end of the reaction. In the case of $[Fe(TPA)(CH_3CN)_2]^{2+}$ (**2**) as catalyst and cyclohexane as substrate, 2.7 TN cyclohexanol (A) and 0.5 TN cyclohexanone (K) are obtained, corresponding to a 32% conversion of the oxidant into organic products. Furthermore, this conversion efficiency is maintained with subsequent addition of more oxidant into the reaction mixture (Fig. 1), demonstrating that **2** is quite a

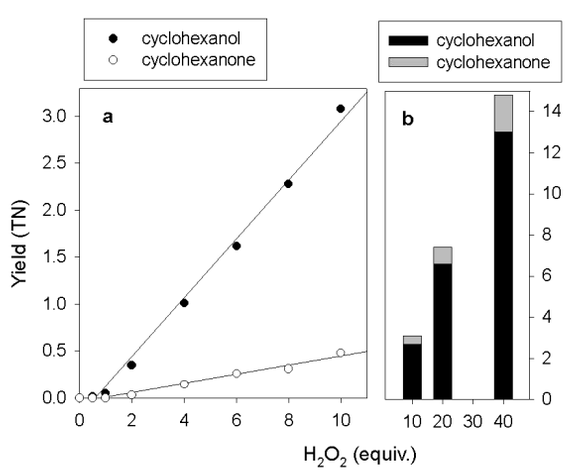

Fig. 1 Product formation on the addition of H_2O_2 into an acetonitrile solution of **2** and cyclohexane in air. Reproduced with permission from the American Chemical Society, publisher of ref. 26.

robust catalyst in alkane hydroxylation, despite the presence of benzylic hydrogens on the ligand framework. More significantly, **2** catalyzes the stereospecific hydroxylation of tertiary C–H bonds of *cis*-1,2-dimethylcyclohexane (Table 1). The major product is (1*R*,2*R* or 1*S*,2*S*)-1,2-dimethylcyclohexanol, the tertiary alcohol with its methyl groups *cis* to each other, its *trans* epimer is not observed. Correspondingly, the only tertiary

Table 1 The oxidation of hydrocarbons with H_2O_2 catalyzed by **1**–**6** and other catalysts

Catalyst	L[g]	Cyclohexane[a,b] A + K	A/K	KIE	Adamantane[c] 3°/2°	*cis*-DMCH[d] RC	Cyclooctene[a,e] D + E	D/E	RC *cis*-2-heptene[f] Epoxide	Diol	Ref.
1	BPMEN	6.3	8	3.2	15	96%	8.4	1 : 8	92%	79%	26, 27
2	TPA	3.2	5	3.5	17	>99%	7.4	1.2 : 1	80%	96%	26, 27
2a		4.3	5				8.1	1 : 1			
3	5-Me_3-TPA	4.0	9	3.8	21	>99%	6.7	1.4 : 1	83%	94%	26, 27
4	6-Me-TPA	4.0	7	3.6	30	85%	4.9	1.3 : 1	69%	95%	26, 27
5	6-Me_2-TPA	2.9	2	4.0	33	64%	6.6	5 : 1	40%	84%	26, 27
6	6-Me_3-TPA	1.4	1	3.3	15	54%	5.6	7 : 1	35%	93%	26, 27
7	N4Py	3.1	1.4	1.5	3.3	27%	0.6	0			23, 44
	$[Fe(TF_4TMAP)]^{5+}$	3.5	16	3.7		>99%	8.5[h]	0			34, 40
	$[Fe^{III}_2(O)(pb)_4(H_2O)_2]^{4+}$	3.6	2.6	3.2	3.5	>99%					47*a*
	$[Fe(cyclam)(O_3SCF_3)_2]$	0					4[h]	0			41
	$HO^{\bullet}$		1	1–2	2	9%					31–33

[a] Yields expressed in mol products per mol catalyst per 10 equiv. H_2O_2. [b] A = cyclohexanol; K = cyclohexanone; KIE = k_H/k_D for cyclohexane hydroxylation. [c] 3°/2° = 3 × (mol 3°-ol)/(mol 2°-ol + mol 2°-one). [d] DMCH = 1,2-dimethylcyclohexane; RC of 3°-ol = 100 × (*trans* − *cis*)/(*cis* + *trans*). [e] D = *cis*-diol; E = epoxide. [f] RC of epoxide or diol product = 100 × (*cis* − *trans*)/(*cis* + *trans*). [g] Ligand abbreviations: cyclam = 1,4,8,11-tetraazacyclotetradecane; pb = (−)-4,5-pinenebipyridine; TF_4TMAPH_2 = meso-tetrakis(2,3,5,6-tetrafluoro-4-*N*,*N*,*N*-trimethylaniliniumyl)porphyrin. [h] Cyclohexene used as substrate.

alcohol product in the oxidation of *trans*-1,2-dimethylcyclohexane is (1*R*,2*S* or 1*S*,2*R*)-1,2-dimethylcyclohexanol, the epimer with the methyl groups *trans* to each other. Indeed, **2** is the first non-heme iron catalyst reported capable of stereospecific alkane hydroxylation with H_2O_2.[22]

Modification of the TPA ligand generates a family of non-heme iron complexes with a range of alkane hydroxylation reactivities (Table 1). Introduction of 5-methyl substituents onto the TPA framework (as in **3**) or one 6-methyl substituent (as in **4**) makes these catalysts somewhat more effective than **2**. However, the presence of two or three 6-methyl substituents in **5** and **6**, respectively, decreases significantly the efficiency of alkane hydroxylation. On the other hand, converting the tripodal TPA framework to that of linear BPMEN affords a catalyst (**1**) that doubles the conversion efficiency of H_2O_2 in cyclohexane oxidation, with the alcohol accounting for 90% of the oxidation products. These results make **1** the most efficient non-heme iron catalyst to date for alkane hydroxylation with H_2O_2 as the oxidant.[24,29]

The alkane hydroxylation reactivity patterns summarized in Table 1 show that catalysts **1**–**6** are far more selective in C–H bond cleavage than $HO^{\bullet}$, a species often implicated in metal/H_2O_2 reactions.[29,30] For all six catalysts, intermolecular kinetic isotope effects (KIE) of 3–4 are observed for cyclohexanol formation, while 3°/2° ratios of 15–33 are found in the competitive oxidation of the tertiary and secondary C–H bonds of adamantane. These values are much larger than those associated with $HO^{\bullet}$-mediated oxidations,[31–33] but comparable to those reported for the heme catalysts, whose chemistry is thought to involve $[(Por^{\bullet})Fe^{IV}{=}O]^{+}$ species.[34–37] Thus, metal-based oxidants similar to the latter are likely to be involved in the reactions of **1**–**6** and H_2O_2.

Despite the similar selectivity in C–H bond cleavage, other reactivity benchmarks divide the six catalysts into two subgroups. For **1**–**4**, designated category A, the alcohol represents a substantial fraction (80–90%) of the cyclohexane oxidation products. Moreover, the hydroxylation of *cis*-1,2-dimethylcyclohexane is highly stereoselective, indicating that alkyl radicals, if formed in the reaction, must be short-lived and react to form the product C–O bond before epimerization, as observed for heme-catalyzed alkane hydroxylations.[13,34,38] In contrast, for **5** and **6**, designated category B, the A/K ratios are much lower and *cis*-1,2-dimethylcyclohexane hydroxylation is much less stereoselective, suggesting the involvement of longer lived radicals in these reactions.

^{18}O Labeling experiments support this categorization (Table 2). When the oxidation of cyclohexane by category A catalysts with 10 equiv. $H_2{}^{16}O_2$ in air is carried out in the presence of 1000 equiv. $H_2{}^{18}O$, the cyclohexanol product shows significant ^{18}O-incorporation from $H_2{}^{18}O$. Complementary experiments with 10 equiv. $H_2{}^{18}O_2$ and 1000 equiv. $H_2{}^{16}O$ show the oxygen atom balance derives from $H_2{}^{18}O_2$, with no involvement of O_2 in these reactions (except for **4**). These results provide evidence for the participation of a metal-based oxidant capable of solvent water exchange. In contrast category B catalysts do not afford alcohol products with ^{18}O from $H_2{}^{18}O$. Instead ^{18}O is incorporated from $H_2{}^{18}O_2$ and $^{18}O_2$. The extent of ^{18}O-incorporation from $^{18}O_2$ into the cyclohexanol product correlates with the loss of stereoselectivity in the hydroxylation of *cis*-1,2-dimethylcyclohexane, consistent with the deduced longer lifetimes of the intermediate alkyl radicals. By the ^{18}O incorporation criterion, **4** appears to represent an intermediate case in which the alcohol product derives its oxygen atom from all three possible sources.

4 Olefin epoxidation and *cis*-dihydroxylation

Complexes **1**–**6** also catalyze the oxidation of olefins (Table 1).[23,25,27] Complex **1** is an excellent epoxidation catalyst, converting 75% of the 10 equiv. H_2O_2 used in cyclooctene oxidation into epoxide product under reaction conditions the same as those for alkane hydroxylation where substrate is present in large excess.[25] The catalyst is also effective under conditions of equimolar substrate and H_2O_2, wherein 0.5% **1** oxidizes 65% of 0.7 M cyclooctene to the epoxide product within 20 minutes. White *et al.* have in fact recently developed reaction conditions that could make this catalyst synthetically useful.[39]

The reactivity patterns of **1**–**6** with respect to olefin epoxidation parallel those observed for alkane hydroxylation.[27] Category A complexes catalyze highly stereoselective olefin epoxidation and incorporate ^{18}O from $H_2{}^{18}O$ into the epoxide product, implicating a metal-based oxidant capable of oxygen-atom exchange with H_2O. In contrast, category B catalysts afford much smaller yields of epoxide with lower stereoselectivity. In fact, the decreased stereoselectivity in *cis*-2-heptene epoxidation correlates with increased amounts of ^{18}O-incorporation from $^{18}O_2$ into cyclooctene oxide, suggesting the involvement of long-lived radical cation intermediates as more 6-methyl substituents are introduced into the ligand framework.

Complexes **1**–**6** also afford an unexpected olefin oxidation product, the *cis*-diol, making them the first examples of iron catalysts capable of olefin *cis*-dihydroxylation, a reaction typically associated with OsO_4. Isolation and characterization of the *cis*-diol products by gas chromatography and NMR

Table 2 ^{18}O-Incorporation from H_2O_2 and H_2O into oxidation products by **1**–**6**[a]

		Cyclohexanol			Cyclooctene oxide		*cis*-Cyclooctane-1,2-diol			
$Fe^{II}L$	L	$H_2{}^{18}O$	$H_2{}^{18}O_2$	$^{18}O_2$	$H_2{}^{18}O$	$H_2{}^{18}O_2$	$^{16}O^{18}O$ from $H_2{}^{18}O$	$^{18}O^{18}O$ from $H_2{}^{18}O$	$^{16}O^{18}O$ from $H_2{}^{18}O_2$	$^{18}O^{18}O$ from $H_2{}^{18}O_2$
1	BPMEN	18(3)	84(4)	—[b]	8(2)	84(1)				
2	TPA	27(2)	70(5)	3(2)	9(1)	90(8)	86(5)	1(1)	97(3)	3(1)
3	5-Me_3-TPA	38(1)	69(1)	—[b]	2(1)	93(6)	83(9)	1(1)	97(3)	2(2)
4	6-Me-TPA	14(4)	62(1)	25(3)	7(1)	71(9)	80(1)	2(1)	94(4)	6(1)
5	6-Me_2-TPA	0	49(2)	54(6)	3(1)	61(8)	3(1)	1(1)	7(1)	93(3)
6	6-Me_3-TPA	1(1)	22(4)	77[b]	3(1)	54(2)	1(1)	0	4(1)	96(1)

[a] Data compiled from refs. 26 and 27. Iron catalyst : H_2O_2 : H_2O : substrate = 1 : 10 : 1000 : 1000 by syringe pump in acetonitrile in the presence of isotopically labeled reagent under ambient atmosphere. [b] Calculated based on the mass balance of oxygen derived from $H_2{}^{18}O$ and $H_2{}^{18}O_2$ experiments.

unequivocally establish their stereochemistry and distinguish them from their *trans* counterparts, which can arise from epoxide ring opening. Furthermore exposure of epoxide to the catalytic reaction conditions results in neither epoxide ring opening nor *cis*-diol formation. Interestingly, unlike for olefin epoxidation by **1**–**6**, olefin dihydroxylations by these catalysts are universally highly stereoselective. Thus epoxidation and *cis*-dihydroxylation appear to be parallel reaction pathways of olefin oxidation by these catalysts.

The preferences of **1**–**6** for olefin epoxidation and *cis*-dihydroxylation again classify them into the same two categories. For category A catalysts, epoxidation represents a significant fraction (40–90%) of the olefin oxidation reactivity; category B catalysts, on the other hand, strongly favor *cis*-dihydroxylation, representing at least 80% of the olefin oxidation activity. In fact, the *cis*-diol/epoxide ratio ranges from 1 : 8 for **1** to 7 : 1 for **6**, a nearly 60-fold change in the outcome of cyclooctene oxidation. Perhaps the feature that dramatically distinguishes the two subgroups is the ^{18}O labeling of the *cis*-diol product (Table 2). For **1**–**4**, one oxygen atom of the diol derives from H_2O_2 while the other comes from water; for **5** and **6**, both diol oxygen atoms derive from H_2O_2. Thus the ligands play an important role in determining the outcome and mechanisms of olefin oxidation.

Other iron catalysts capable of stereospecific alkane hydroxylation and/or olefin epoxidation with H_2O_2 as oxidant do not carry out olefin *cis*-dihydroxylation. This list includes iron porphyrin complexes,[12,13,34,40] $[Fe(cyclam)(O_3SCF_3)_2]$,[41] and iron bleomycin and its analogues.[42,43] Furthermore $[Fe(N4Py)(CH_3CN)]^{2+}$ (**7**), a complex structurally closely related to **2** by virtue of having an additional pendant pyridine ligand (Scheme 2), does not catalyze olefin oxidation at all.[23,44] We have previously noted that what distinguishes **1**–**6** structurally from these other iron complexes is the presence of two labile coordination sites positioned *cis* to each other (Scheme 2).[23] In the next section, we will discuss how this structural feature plays a significant role in activating the peroxo O–O bond to elicit the novel chemistry catalyzed by this family of complexes.

5 Mechanism for Fe(TPA) catalysis

Complex **2** is representative of category A catalysts, whose mechanism of action has been studied in the greatest detail. Scheme 3 shows the overall mechanism proposed for the catalytic cycle of **2** which postulates the participation of Fe^{III}–OH, Fe^{III}–OOH, and Fe^{V}=O species.

The iron(II) complexes used in this study are convenient precursors for the Fe^{III}–OH species, which is readily accessible by oxidation with half an equivalent of H_2O_2. The Fe^{III}–OH species in turn readily generates by ligand exchange the Fe^{III}–OOH species, the first key intermediate of this catalytic cycle. Support for this scheme can be found in Fig. 1, which shows that cyclohexanol and cyclohexanone are produced linearly as a function of added H_2O_2 in the **2**-catalyzed oxidation of cyclohexane, but only after the addition of the first 0.5 equiv H_2O_2. A similar reaction profile is observed in the **2**-catalyzed epoxidation and *cis*-dihydroxylation of cyclooctene.[27] Upon addition of the first 0.5 equiv. H_2O_2 to a solution of **2**, the sharp NMR features of diamagnetic **2** in the 0–11 ppm region are immediately replaced by broader peaks spanning up to 40 ppm in shift characteristic of a $(TPA)_2Fe^{III}{}_2(\mu\text{-}O)$ complex,[45] the thermodynamic sink for Fe^{III}–OH complexes.[46] In support, $[Fe^{III}{}_2O(TPA)_2(H_2O)_2](ClO_4)_4$ (**2a**) has a catalytic efficiency and product distribution comparable to that of **2** for both alkane hydroxylation and olefin oxidation (Table 1). However unlike for **2**, there is no lag phase observed in product formation for **2a**. Thus both **2** and **2a** are excellent catalysts for hydrocarbon oxidation.

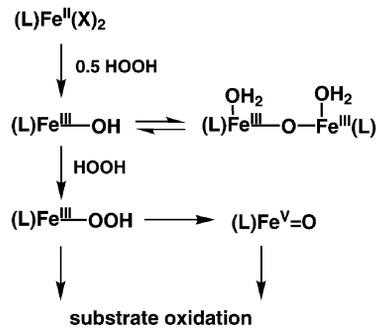

Scheme 3 Conversion of precursor iron complexes into active intermediates.

The excellent catalytic efficiency of **2** and **2a** contrasts the reactivity of other Fe^{III}(TPA) complexes, which are *not* catalysts for hydrocarbon oxidation. For example, no products are observed when $[Fe(TPA)Cl_2](ClO_4)$, $[Fe(TPA)Br_2](ClO_4)$, or $[Fe_2O(TPA)_2(O_2CR)](ClO_4)_3$, is used as the catalyst under conditions that elicit cyclohexane oxidation by **2** and **2a**. We attribute the lack of reactivity to the absence of weakly coordinated ligands that can be readily displaced by H_2O_2 to efficiently generate the Fe^{III}–OOH species responsible for the novel metal-centered hydrocarbon oxidation chemistry discussed in this paper. A similar ligand effect has also been reported for a related system by Mekmouche *et al.*[47b]

The reaction of **2** or **2a** with excess H_2O_2 at −40 °C leads to the observation of a transient species, which has been characterized by a number of spectroscopic techniques to be a low-spin Fe^{III}–η^1-OOH intermediate (Fig. 2).[22,48] Most significant among these observations from a mechanistic perspective is its resonance Raman spectrum, which exhibits features at 626 and 789 cm^{-1} assigned to ν(Fe–OOH) and ν(O–O) modes, respectively. The values for ν(Fe–OOH) and ν(O–O) are respectively higher and lower than corresponding values found for high-spin iron-peroxo complexes,[49] implying that the presence of the low-spin iron(III) center strengthens the Fe–O bond and weakens the

O–O bond. Lehnert *et al.* provide strong support for this notion in their detailed spectroscopic analysis of the related $[Fe^{III}(TPA)(OO^tBu)]^{2+}$ intermediate.[50] DFT calculations on the putative low-spin Fe^{III}–OOH species in the catalytic cycle of cytochrome P450 also come to the same conclusion.[51] Thus the low-spin iron(III) center activates the O–O bond for cleavage.

It should be noted that the $[Fe^{III}(TPA)(OOH)]^{2+}$ species, though minimally formulated to appear as a five-coordinate complex, must have a sixth ligand to be consistent with the low-spin nature of the iron(III) center. This sixth ligand is likely to be CH_3CN or H_2O, which could be readily dissociated in the course of the mass spectrometry experiment. From experiments carried out in the presence of $H_2{}^{18}O$, it is clear that the bound hydroperoxide cannot exchange its oxygen atoms with bound or solvent $H_2{}^{18}O$, as spectroscopic features associated with the Fe^{III}–OOH species in both resonance Raman and electrospray ionization mass spectra are unchanged under these conditions. Thus the O–O bond of the hydroperoxo intermediate remains intact at this stage of characterization.

Subsequent reaction of the $[Fe^{III}(TPA)(OOH)]^{2+}$ intermediate with hydrocarbons results in product formation with high stereoselectivity. Three possible pathways immediately come to mind. The Fe^{III}–OOH intermediate itself can directly transfer an oxygen atom to substrate, as is proposed for early transition metal peroxo complexes, or it may decompose by O–O bond lysis generating oxidants that react with the substrate. O–O bond heterolysis would generate a formally Fe^{V}=O species, while homolysis would form an Fe^{IV}=O species and the highly reactive HO$^{\bullet}$. The highly selective oxidations observed for category A catalysts effectively exclude the homolysis pathway, leaving only direct attack by Fe^{III}–OOH and O–O bond heterolysis pathways as viable mechanistic options (Scheme 4).

It should be noted that complex **7** also reacts with H_2O_2 to form a transient low-spin Fe^{III}–OOH intermediate, with spectral properties quite similar to that derived from **2**.[48,52] However **7** does not catalyze the highly stereoselective hydrocarbon oxidation chemistry noted for **2** and the Fe^{III}–OOH species is in fact proposed to undergo O–O bond homolysis in its mechanism of hydrocarbon oxidation.[44] Thus the presence of the additional pendant pyridine ligand in **7** dramatically alters the course of O–O bond cleavage.

Strong evidence for the participation of the O–O bond heterolysis pathway for category A catalysts derives from experiments carried out in the presence of $H_2{}^{18}O$, which show oxidation products with ^{18}O incorporation (Table 2).[24,26,27] The observed ^{18}O incorporation from $H_2{}^{18}O$ cannot be accounted for by the direct insertion pathway and requires a mechanism that allows ^{18}O exchange of the oxidant with solvent water prior to substrate attack. This exchange is most easily rationalized by invoking a formally Fe^{V}=O species derived from O–O bond heterolysis, analogous to that in heme-catalyzed oxidations.[13,38] For the latter, oxygen incorporation from solvent water occurs *via* coordination of water to the iron center *trans* to the oxo group and subsequent "oxo-hydroxo tautomerization".[53] For the Fe(TPA) catalyst, we have proposed that this ^{18}O exchange occurs by the sequence of steps shown in Scheme 4: a) coordination of $H_2{}^{18}O$ to the low-spin Fe^{III}–OOH intermediate and formation of a hydrogen-bonded five-membered ring intermediate, b) loss of water leading to O–O bond heterolysis, and c) oxo–hydroxo tautomerization prior to attack of substrate.

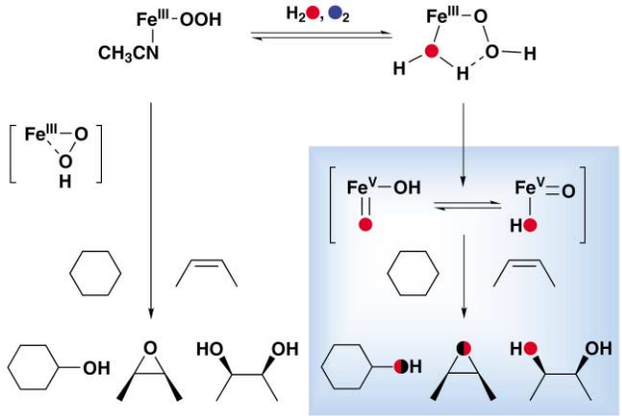

Scheme 4 Mechanistic scheme for category A catalysts.

The existence of a water binding pre-equilibrium in step a is demonstrated by the fact that the extent of ^{18}O labeling in the oxidation products depends on the amount of $H_2{}^{18}O$ present in the reaction mixture.[26,27] Fig. 3 displays the results of a series of cyclohexane hydroxylation experiments conducted using catalyst **3**, showing that the fraction of R^{18}OH increases linearly at

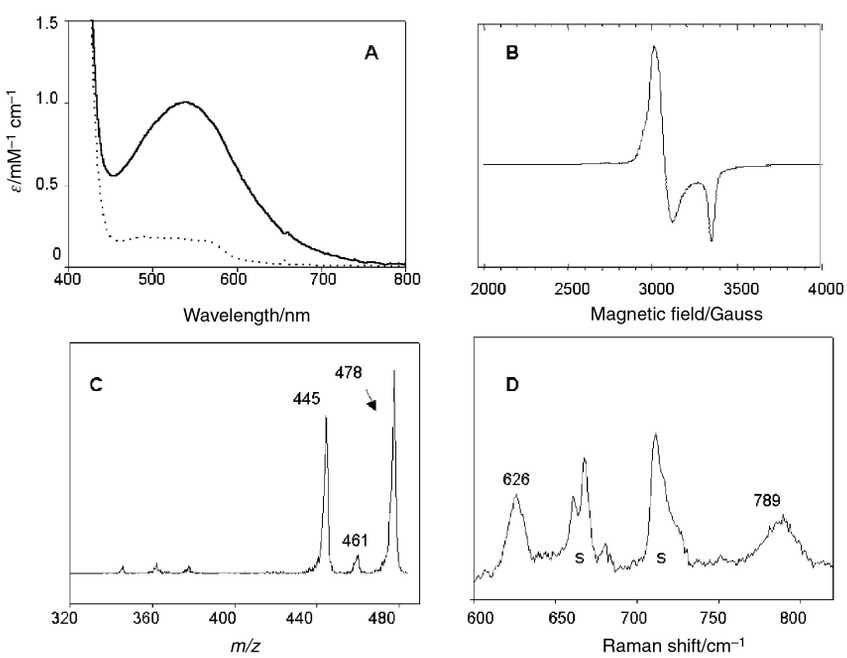

Fig. 2 Spectroscopic characterization of the $[Fe(TPA)(OOH)]^{2+}$ intermediate: A) electronic absorption spectrum in CH_3CN (solid line) compared with that of $[Fe(TPA)(CH_3CN)_2]^{2+}$ (dashed line); B) EPR spectrum; C) electrospray ionization mass spectrum; D) resonance Raman spectrum (solvent peaks are marked with s). Reproduced with permission from Elsevier, the publisher of ref. 29.

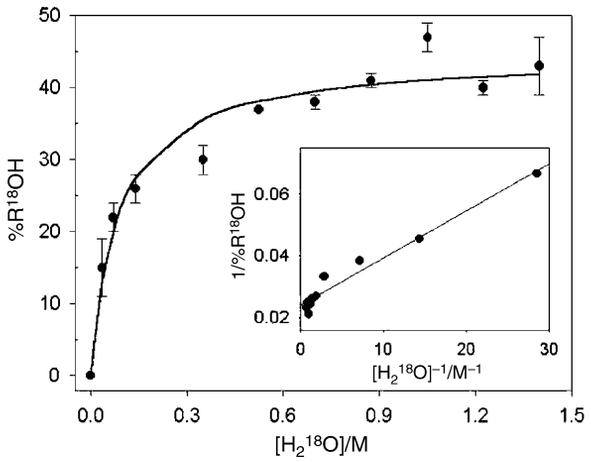

Fig. 3 Plot of the fraction of ^{18}O-labeled alcohol (%R^{18}OH) obtained in cyclohexane hydroxylation by **3**/H_2O_2 as a function of the concentration of $H_2{}^{18}O$ ([$H_2{}^{18}O$]). Inset: the corresponding double-reciprocal plot. Reproduced with permission from the American Chemical Society, publisher of ref. 26.

lower $H_2{}^{18}O$ concentrations as $H_2{}^{18}O$ concentration is increased but reaches a plateau at higher $H_2{}^{18}O$ concentrations. Similar saturation curves are found for the formation of ^{18}O-labeled epoxide and *cis*-diol in the oxidation of cyclooctene by catalyst **2**. Double reciprocal plots of the data afford an estimate of 15–30 M^{-1} for the association constant of H_2O. A similar saturation behavior for ^{18}O incorporation from water has been found in heme-catalyzed oxidations.[10,54]

The partial incorporation of ^{18}O from water into the alcohol and epoxide products of **2**-catalyzed oxidations may reflect two factors: 1) the partitioning between the direct insertion and the O–O bond heterolysis pathways in the oxidation, and 2) the extent of oxo–hydroxo tautomerization. The data available does not allow us to provide a more quantitative assessment of their relative contributions. However the *cis*-diol labeling results showing the incorporation of one atom of oxygen from H_2O and the other atom of oxygen from H_2O_2 clearly demonstrate that the O–O bond heterolysis pathway is essentially the only dihydroxylation mechanism in the presence of excess water. This observation lends strong credence to the validity of Scheme 4.

6 Tuning the reactivity of the iron catalyst with 6-methyl substitution

As evidenced from the entries in Tables 1 and 2, the introduction of 6-methyl substituents affects considerably the course of hydrocarbon oxidation by this family of catalysts. First of all, category B catalysts carry out alkane hydroxylation and generate transient alkyl radicals that are long enough lived to undergo epimerization or trapping by O_2, despite the fact that cyclohexane/cyclohexane-d_{12} and adamantane 3°/2° competition experiments indicate an oxidant as selective as that for category A catalysts.[26] Secondly, category B catalysts oxidize olefins predominantly to *cis*-diols.[27] Lastly, oxidation products of catalysts in this category do not incorporate ^{18}O from water.[26,27] Thus the mechanism proposed in Scheme 4 for category A catalysts must be modified somewhat in order to apply to category B catalysts.

The introduction of 6-methyl substituents onto the TPA ligand framework favors the high-spin state for the iron center due to the steric effects of the 6-methyl group that restrict the extent to which the metal ion cavity can shrink.[28] This preference has been demonstrated in the crystal structures of the series of $[Fe(L)(CH_3CN)_2]^{2+}$ complexes and the EPR spectra of the series of $[Fe^{III}(L)(OO^tBu)]^{2+}$ complexes. The iron(III) center is low-spin for the parent TPA complex and high-spin for the 6-Me_2-TPA and 6-Me_3-TPA complexes, while the 6-Me-TPA complex consists of a mixture of low-spin and high-spin species. Given these precedents, the key Fe^{III}–OOH intermediate for category B catalysts must be high-spin.

A comparison of resonance Raman data suggests that the O–O bond in a high-spin iron(III)-peroxo complex is not as activated for cleavage as that found for its low-spin counterpart.[28,50] Furthermore, the lack of ^{18}O incorporation from $H_2{}^{18}O$ into any of the oxidation products indicates that the five-membered ring intermediate proposed for the category A catalysts is unlikely to form in the case of category B catalysts, perhaps because of steric hindrance. Thus the stronger O–O bond of the high-spin iron(III)-peroxo intermediate needs further activation. The observed requirement for two *cis* labile sites in the catalysis of *cis*-dihydroxylation[23,27] leads us to postulate the isomerization of the Fe^{III}–η^1-OOH intermediate to an η^2-OOH species, as shown in Scheme 5. This Fe^{III}–η^2-OOH species would in turn

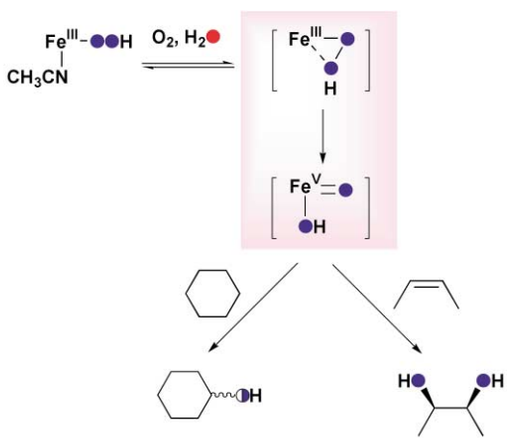

Scheme 5 Mechanistic scheme for category B catalysts.

then either react directly with the olefin to form the *cis*-diol product or convert to a *cis*-HO–Fe^v=O species prior to olefin attack to parallel the chemistry of the low-spin η^1-OOH intermediates. However, the nearly insignificant amount of ^{18}O-incorporation from H_2O into the diol product suggests that either a *cis*-HO–Fe^V=O species is not involved or that $H_2{}^{18}O$ exchange with the high-valent species does not occur, presumably due to the presence of the 6-methyl substituents.

The observation that the catalytic behavior associated with **4** is intermediate between those of categories A and B may be rationalized by the fact that complex **4** gives rise to a mixture of low-spin and high-spin iron(III)-peroxo species that react with substrate in distinct ways.[28] For example in alkane hydroxylation, the incorporation of 14% ^{18}O from $H_2{}^{18}O$ into cyclohexanol (compared to 27% for **2**) may be attributed to the H^{18}O–Fe^V=O species derived from the low-spin peroxo intermediate, while the incorporation of 25% ^{18}O from $^{18}O_2$ into cyclohexanol (compared to 77% for **6**) and lower stereoselectivity of *cis*-1,2-dimethylcyclohexane hydroxylation may be attributed to the longer lived alkyl radicals produced by the corresponding high-spin intermediate. The extents of ^{18}O incorporation observed suggest that the two intermediates are comparably reactive towards alkanes. On the other hand, olefin oxidation by **4** appears to follow the patterns of category A catalysts more closely, so the low-spin peroxo intermediate may be somewhat more reactive towards alkenes.

Lastly, it should be noted that spectroscopic evidence for none of the intermediates in colored boxes in Schemes 4 and 5 is available. These various reactive species, however plausible, are to date all mechanistic speculations that derive indirectly from experimental observations. Nevertheless these notions serve as a useful framework within which to understand the

differences in the hydrocarbon oxidation activities among the catalysts in this family.

7 Summary and bioinorganic relevance

In this perspective, we have summarized the catalytic properties of a family of non-heme iron(II) complexes which use H_2O_2 as oxidant to carry out alkane hydroxylation, olefin epoxidation, and olefin *cis*-dihydroxylation, in many cases with high stereoselectivity. These reactions occur *via* transient Fe^{III}–OOH species whose spin states can be tuned by the degree of 6-methyl substitution on the ligand framework. These differing spin states are the key to the range of reactivities observed. Category A complexes give rise to low-spin Fe^{III}–OOH intermediates and catalyze alkane hydroxylation, olefin epoxidation, and olefin *cis*-dihydroxylation with high stereoselectivity. The oxidation mechanism involves a species that allows solvent water to be incorporated into the products. Category B complexes, on the other hand, give rise to high-spin Fe^{III}–OOH intermediates. Alkane hydroxylation proceeds with much lower stereoselectivity due to the generation of long-lived alkyl radicals, but olefin oxidation leads predominantly to *cis*-dihydroxylation wherein both atoms of the H_2O_2 are incorporated into the *cis*-diol product.

A common feature of this family of catalysts is the use of tetradentate ligands that afford metal centers with two *cis* labile sites. This structural requirement is particularly stringent for olefin *cis*-dihydroxylation, as demonstrated by the lack of this reactivity for complexes with two *trans* labile sites such as porphyrin complexes and $[Fe(cyclam)(O_3SCF_3)_2]$, even though they are excellent catalysts for stereospecific alkane hydroxylation and/or olefin epoxidation (Table 1).[12,13,34,38,40,41] Furthermore, with only one labile site, $[Fe(N4Py)(CH_3CN)]^{2+}$ (**7**) does not catalyze stereospecific alkane hydroxylation and olefin oxidations, despite the fact that **2** and **7** are quite closely related in structure (Scheme 2) and both afford low-spin Fe^{III}–OOH intermediates that are spectroscopically quite similar.[23,44,48] We have speculated that one labile site is needed to bind the hydroperoxide, while the adjacent site is required for O–O activation. For category A catalysts, we have compelling evidence from ^{18}O labeling studies for the binding of H_2O at this adjacent site leading to O–O bond heterolysis to form a *cis*-HO–Fe^{V}=O species (Scheme 4). However for category B catalysts, the evidence for the participation of a *cis*-HO–Fe^{V}=O species in reactions is equivocal. Nevertheless we suggest that the adjacent site is required for the formation of an Fe^{III}–η^2-OOH en route to the *cis*-HO–Fe^{V}=O species in the mechanism (Scheme 5).

The studies discussed above thus provide a synthetic precedent for invoking a formally Fe^{V}=O species in the oxygen activation mechanisms postulated for non-heme iron enzymes such as methane monooxygenase and Rieske dioxygenases. For methane monooxygenase, the $Fe^{IV}_2(\mu\text{-}O)_2$ core associated with key intermediate **Q**[18] is proposed to isomerize to an Fe^{III}–O–Fe^{V}=O unit prior to its attack on the methane C–H bond.[55,56] For Rieske dioxygenases, the key oxidant must be a mononuclear iron species capable of the *cis*-dihydroxylation of arene double bonds as well as the highly stereoselective hydroxylation of aliphatic C–H bonds with ^{18}O incorporation from $H_2{}^{18}O$.[57,58] A *cis*-HO–Fe^{V}=O species like that postulated for the TPA catalysts would seem to be the best candidate to rationalize all these results.[3] It should be noted that the evidence derived from our studies is mechanistic, rather than by direct spectroscopic observation. Furthermore, the all-nitrogen ligand environments of BPMEN and TPA ligands may not necessarily reproduce the electronic effects exerted by the combination of histidine and carboxylate ligands found in these non-heme iron enzymes. Thus further studies, both experimental and computational, are needed to clarify the precise nature of such formally Fe^{V}=O species.

Our studies also suggest a basis with which to rationalize Nature's choice of ligand environments for carrying out iron-catalyzed hydrocarbon oxidations. With five principally nitrogenous ligands, the mononuclear iron centers of cytochrome P450[7] and the iron requiring antitumor drug bleomycin[59] generate low-spin Fe^{III}–OOH intermediates,[60,61] which play an important role in the stereospecific alkane hydroxylation and/or olefin epoxidation associated with these systems. On the other hand, the arene *cis*-dihydroxylating Rieske dioxygenases have a mononuclear iron site coordinated to two histidines and a bidentate aspartate, with two adjacent sites available for exogenous ligands,[20] a ligation geometry that corresponds to that observed for our synthetic catalysts. Given the presence of the 2-His-1-carboxylate facial triad motif in the enzymes,[62] it is likely that the postulated[3,21] but as yet unobserved Fe^{III}–OOH intermediate would be high-spin. The proposed participation of a high-spin Fe^{III}–OOH species in the catalytic cycle would be consistent with our observation that synthetic catalysts with high-spin centers favor olefin *cis*-dihydroxylation over epoxidation.

Finally our studies have uncovered a diverse range of hydrocarbon oxidation reactivities accessible by simple tuning of one ligand framework. These ligand effects control the mode of O–O bond cleavage, modulate the lifetimes of radicals produced in the course of the reaction, and determine whether one or two oxygen atoms are transferred from oxidant to substrate. These seemingly subtle changes in ligand structure can lead to rather dramatic differences in the outcome of hydrocarbon oxidation, thereby posing a challenge to bioinorganic chemists to gain a better understanding of this complex reaction surface.

Acknowledgements

This work was supported by a National Institutes of Health MERIT award to L. Q. (GM-33162), a thesis fellowship to K. C. from the Department of Chemistry of the University of Minnesota, and a postdoctoral fellowship to M. C. from the Fundacio La Caixa.

References

1 J. S. Valentine, C. S. Foote, A. Greenberg and J. F. Liebman, eds., *Active Oxygen in Biochemistry*, Chapman and Hall, Glasgow, 1995.
2 B. J. Wallar and J. D. Lipscomb, *Chem. Rev.*, 1996, **96**, 2625.
3 L. Que, Jr. and R. Y. N. Ho, *Chem. Rev.*, 1996, **96**, 2607.
4 M. Sono, M. P. Roach, E. D. Coulter and J. H. Dawson, *Chem. Rev.*, 1996, **96**, 2841.
5 E. I. Solomon, T. C. Brunold, M. I. Davis, J. N. Kemsley, S.-K. Lee, N. Lehnert, F. Neese, A. J. Skulan, Y.-S. Yang and J. Zhou, *Chem. Rev.*, 2000, **100**, 235.
6 D. T. Gibson, ed., *Microbial Degradation of Organic Molecules*, Marcel Dekker, New York, 1984.
7 P. R. Ortiz de Montellano, ed., *Cytochrome P450. Structure, Mechanism and Biochemistry*, 2nd edn., Plenum Press, New York, 1995.
8 J. M. Pratt, T. I. Ridd and L. J. King, *J. Chem. Soc., Chem. Commun.*, 1995, 2297.
9 A. D. N. Vaz, S. J. Pernecky, G. M. Raner and M. J. Coon, *Proc. Natl. Acad. Sci. USA*, 1996, **93**, 4644.
10 K. A. Lee and W. Nam, *J. Am. Chem. Soc.*, 1997, **119**, 1916.
11 M. Newcomb and P. H. Toy, *Acc. Chem. Res.*, 2000, **33**, 449.
12 W. Nam, M. H. Lim, H. J. Lee and C. Kim, *J. Am. Chem. Soc.*, 2000, **122**, 6641.
13 W. Nam, M. H. Lim, S. K. Moon and C. Kim, *J. Am. Chem. Soc.*, 2000, **122**, 10805.
14 S.-K. Lee, J. C. Nesheim and J. D. Lipscomb, *J. Biol. Chem.*, 1993, **268**, 21569.
15 K. E. Liu, A. M. Valentine, D. Wang, B. H. Huynh, D. E. Edmondson, A. Salifoglou and S. J. Lippard, *J. Am. Chem. Soc.*, 1995, **117**, 10174.
16 M. Merkx, D. A. Kopp, M. H. Sazinsky, J. L. Blazyk, J. Müller and S. J. Lippard, *Angew. Chem., Int. Ed.*, 2001, **40**, 2782.

17 N. Elango, R. Radhakrishnan, W. A. Froland, B. J. Wallar, C. A. Earhart, J. D. Lipscomb and D. H. Ohlendorf, *Protein Sci.*, 1997, **6**, 556.
18 L. Shu, J. C. Nesheim, K. Kauffmann, E. Münck, J. D. Lipscomb and L. Que, Jr., *Science*, 1997, **275**, 515.
19 S. M. Resnick and D. T. Gibson, *J. Ind. Microbiol.*, 1996, **17**, 438.
20 B. Kauppi, K. Lee, E. Carredano, R. E. Parales, D. T. Gibson, H. Eklund and S. Ramaswamy, *Structure*, 1998, **6**, 571.
21 M. D. Wolfe, J. V. Parales, D. T. Gibson and J. D. Lipscomb, *J. Biol. Chem.*, 2001, **276**, 1945.
22 C. Kim, K. Chen, J. Kim and L. Que, Jr., *J. Am. Chem. Soc.*, 1997, **119**, 5964.
23 K. Chen and L. Que, Jr., *Angew. Chem., Int. Ed.*, 1999, **38**, 2227.
24 K. Chen and L. Que, Jr., *Chem. Commun.*, 1999, 1375.
25 M. Costas, A. K. Tipton, K. Chen, D.-H. Jo and L. Que, Jr., *J. Am. Chem. Soc.*, 2001, **123**, 6722.
26 K. Chen and L. Que, Jr., *J. Am. Chem. Soc.*, 2001, **123**, 6327.
27 K. Chen, M. Costas, J. Kim, A. K. Tipton and L. Que, Jr., *J. Am. Chem. Soc.*, accepted.
28 Y. Zang, J. Kim, Y. Dong, E. C. Wilkinson, E. H. Appelman and L. Que, Jr., *J. Am. Chem. Soc.*, 1997, **119**, 4197.
29 M. Costas, K. Chen and L. Que, Jr., *Coord. Chem. Rev.*, 2000, **200–202**, 517.
30 K. U. Ingold and P. A. MacFaul, in *Biomimetic Oxidations Catalyzed by Transition Metal Complexes*, ed. B. Meunier, Imperial College Press, London, 2000, pp. 45–89.
31 A. F. Trotman-Dickenson, *Adv. Free Radical Chem.*, 1965, **1**, 32.
32 S. Miyajima and O. Simamura, *Bull. Chem. Soc. Jpn.*, 1975, **48**, 526.
33 G. V. Buxton, C. L. Greenstock, W. P. Helman and A. B. Ross, *J. Phys. Chem. Ref. Data*, 1988, **17**, 513.
34 W. Nam, Y. M. Goh, Y. J. Lee, M. H. Lim and C. Kim, *Inorg. Chem.*, 1999, **38**, 3238.
35 J. T. Groves and T. E. Nemo, *J. Am. Chem. Soc.*, 1983, **105**, 6243.
36 A. M. Khenkin and A. E. Shilov, *New J. Chem.*, 1989, **13**, 659.
37 A. B. Sorokin and A. M. Khenkin, *New J. Chem.*, 1990, **14**, 63.
38 J. T. Groves and Y.-Z. Han, in *Cytochrome P450: Structure, Mechanism, and Biochemistry*, ed. P. R. Ortiz de Montellano, Plenum Press, New York, 1995, pp. 3–48.
39 M. C. White, A. G. Doyle and E. N. Jacobsen, *J. Am. Chem. Soc.*, 2001, **123**, 7194.
40 W. Nam, H. J. Han, S.-Y. Oh, Y. J. Lee, M.-H. Choi, S.-Y. Han, C. Kim, S. K. Woo and W. Shin, *J. Am. Chem. Soc.*, 2000, **122**, 8677.
41 W. Nam, R. Y. N. Ho and J. S. Valentine, *J. Am. Chem. Soc.*, 1991, **113**, 7052.
42 D. C. Heimbrook, S. A. Carr, M. A. Mentzer, E. C. Long and S. M. Hecht, *Inorg. Chem.*, 1987, **26**, 3835.
43 R. J. Guajardo, S. E. Hudson, S. J. Brown and P. K. Mascharak, *J. Am. Chem. Soc.*, 1993, **115**, 7971.
44 G. Roelfes, M. Lubben, R. Hage, L. Que, Jr. and B. L. Feringa, *Chem. Eur. J.*, 2000, **6**, 2152.
45 R. E. Norman, S. Yan, L. Que, Jr., J. Sanders-Loehr, G. Backes, J. Ling, J. H. Zhang and C. J. O'Connor, *J. Am. Chem. Soc.*, 1990, **112**, 1554.
46 D. M. Kurtz, Jr., *Chem. Rev.*, 1990, **90**, 585.
47 (*a*) Y. Mekmouche, C. Duboc-Toia, S. Ménage, C. Lambeaux and M. Fontecave, *J. Mol. Catal. A: Chem.*, 2000, **156**, 85; (*b*) Y. Mekmouche, S. Ménage, C. Toia-Duboc, M. Fontecave, J.-B. Galey, C. Lebrun and J. Pecaut, *Angew. Chem., Int. Ed.*, 2001, **40**, 949.
48 R. Y. N. Ho, G. Roelfes, B. L. Feringa and L. Que, Jr., *J. Am. Chem. Soc.*, 1999, **121**, 264.
49 J.-J. Girerd, F. Banse and A. J. Simaan, *Struct. Bonding (Berlin)*, 2000, **97**, 143.
50 (*a*) N. Lehnert, R. Y. N. Ho, L. Que, Jr. and E. I. Solomon, *J. Am. Chem. Soc.*, 2001, **123**, 8271; (*b*) N. Lehnert, R. Y. N. Ho, L. Que, Jr. and E. I. Solomon, *J. Am. Chem. Soc.*, 2001, **123**, in press.
51 D. L. Harris and G. H. Loew, *J. Am. Chem. Soc.*, 1998, **120**, 8941.
52 M. Lubben, A. Meetsma, E. C. Wilkinson, B. Feringa and L. Que, Jr., *Angew. Chem., Int. Ed. Engl.*, 1995, **34**, 1512.
53 J. Bernadou and B. Meunier, *Chem. Commun.*, 1998, 2167.
54 M. H. Lim, Y. J. Lee, Y. M. Goh, W. Nam and C. Kim, *Bull. Chem. Soc. Jpn.*, 1999, **72**, 707.
55 P. E. M. Siegbahn and R. H. Crabtree, *J. Am. Chem. Soc.*, 1997, **119**, 3103.
56 P. E. M. Siegbahn, R. H. Crabtree and P. Nordlund, *J. Biol. Inorg. Chem.*, 1998, **3**, 314.
57 D. T. Gibson, S. M. Resnick, K. Lee, J. M. Brand, D. S. Torok, L. P. Wackett, M. J. Schocken and B. E. Haigler, *J. Bacteriol.*, 1995, **177**, 2615.
58 L. P. Wackett, L. D. Kwart and D. T. Gibson, *Biochemistry*, 1988, **27**, 1360.
59 J. Stubbe and J. W. Kozarich, *Chem. Rev.*, 1987, **87**, 1107.
60 R. Davydov, T. M. Makris, V. Kofman, D. E. Werst, S. G. Sligar and B. M. Hoffman, *J. Am. Chem. Soc.*, 2001, **123**, 1403.
61 R. M. Burger, T. A. Kent, S. B. Horwitz, E. Münck and J. Peisach, *J. Biol. Chem.*, 1983, **258**, 1559.
62 E. L. Hegg and L. Que, Jr., *Eur. J. Biochem.*, 1997, **250**, 625.